Multi-Point Turn Decision Making Framework for Human-Like Automated Driving

Chun-Wei Chang[1], Chen Lv[1], Huaji Wang[1], Hong Wang[2], Dongpu Cao[1], Efstathios Velenis[1], Fei-Yue Wang[3]
[1]Advanced Vehicle Engineering Centre, Cranfield University, Bedford, United Kingdom
[2]Department of Mechanical and Mechatronics Engineering, University of Waterloo, Waterloo, Canada
[3]Qingdao Academy of Intelligent Industries, Qingdao, China
[1]{c.chang, c.lyu, huaji.wang, d.cao, e.velenis}@cranfield.ac.uk; [2]wanghongbit@gmail.com; [3]feiyue.wang@ic.ac.cn

***Abstract*—This paper proposes a new methodology of achieving human-like automated driving, and presents a decision making framework and the minimum thresholds of the occupied widths of multi-point turn for autonomous vehicles. The concept of human-like automated driving and the multi-point turn decision making framework for autonomous vehicles are proposed at first. Then, the geometric characteristics that are provided by the reference paths of turn around manoeuvres are analysed. The minimum operation widths from U Turn to Five-Point Turn are investigated respectively, and the methodology and results are then generalized to solve the multi-point turn (i.e. N-Point Turn) scenario. Finally, by using the derived results and characteristics analysed above, the functions that are able to evaluate the most feasible turn around manoeuvre within the current situation are provided.**

Keywords—human-like automated driving; turn around manoeuvre; multi-point turn; decision making.

I. INTRODUCTION

The on-vehicle automation system is primarily developed to replace the human driver in driving tasks in order to enhance the driving performance and traffic efficiency [1]-[7] and avoid the possible fatalities [8]-[12] (e.g. correcting manipulation mistakes, reducing the traffic crashes related to human behaviours and decisions, etc.). However, most published researches neglect that the human imperfection and preference not always leads to negative consequences. An explicit example is the motion sickness, which has been confirmed that it is one of the primary after-effects while riding an autonomous vehicle [13]-[16]. In order to mitigate the undesired influence and increase the public acceptance, a functionality which is able to imitate the behaviours of human drivers on the premise of safety is required. This paper aims to deliver the preliminary effort of achieving the human-like turn around automated driving.

Being one of the common vehicle driving scenarios in both rural and urban area, the turning manoeuvre has been researched for over twenty years [17], [18]. Turn around is a specific version of turning manoeuvres, and can be seen as a general terminology that describes the vehicle behaviours while reorienting to the opposite heading direction. This manoeuvre is often executed under emergent or unexpected situations; for instance, driving into a dead end street, avoiding front obstacles and traffic [19], interrupting by a higher-priority driving mission, redirecting to the new destination, etc. As the pioneer in developing autonomous vehicles, Google realises that turn around is one of the trickiest driving tasks even for a professional driver to master. Therefore, Google Cars are assigned to execute hundreds of multi-point turns per week with the purpose of improving the performance while operating these difficult driving manoeuvres [20].

Since the heading direction of a vehicle can be adjusted through steering the front wheels during forward or backward movements, turn around manoeuvres can be divided into two categories: One enables the vehicle to achieve target (i.e. turn 180 degrees) without any transition between forward driving and reversing, including detours and U Turn; the other is comprised of multiple forward and backward reorientations, which is so called N-Point Turn. Apart from the former has the possibility to provide efficient performance but requires a broad area, the latter can be manipulated within the permitted width less than two standard traffic lanes.

This paper presents a multi-point turn decision making framework and derives the related minimum thresholds of the occupied widths; the reference paths are referred to the Reeds-Shepp path [21] so as to approach human-like behaviours that drivers prefer to make a brief stop while operating the hand steering wheel from one direction to the other. The remaining sections of the paper are organised as follows. Section II introduces the human-like automated driving framework and the multi-point turn decision making flowchart for autonomous vehicles. Section III remarks the geometric characteristics that are followed by the reference paths of multi-point turn and derives the minimum operation widths from U Turn to Five-Point Turn respectively, which can be generalized to N-Point Turn. By taking advantage of the outcomes which are acquired from the prior derivations, two equations that calculate the minimum number of multi-point turn based on the environmental information are provided in Section IV. Finally, the contributions of this paper are concluded in Section V.

II. PROPOSED FRAMEWORKS

Fig. 1 presents the framework for achieving human-like automated driving. The concept of human-like automated driving can be primarily divided into three parts, which are

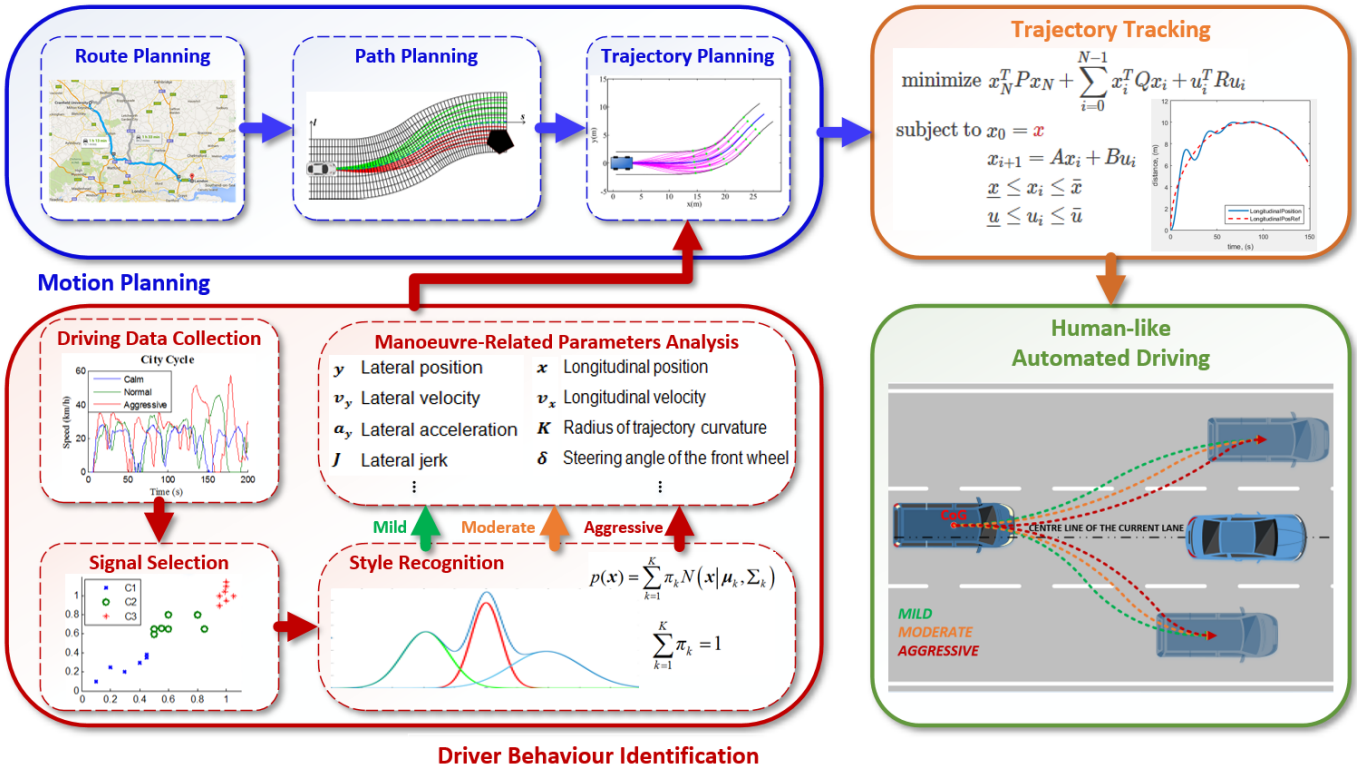

Fig. 1. The general framework for an autonomous vehicle to achieve human-like automated driving.

the motion planning, the driver behaviour identification and the tracking control. In the motion planning section, the target is to utilise existed planning techniques to generate the vehicle-dynamics-based trajectory of the determined driving task [5], [9], [22]-[24]. On the other hand, the purpose of the driver behaviour identification part is to classify the real driving data from human drivers into selected number of different driving styles (e.g. Aggressive, Moderate, and Mild) through machine learning techniques [25]. Once the values of style-related parameters are generated, the results will be combined with the vehicle-dynamics-based trajectory in the motion planning section to modify relevant variables and enable the trajectory planner to provide human-like trajectories. Finally, the control algorithm tracks the trajectories of different driving styles in the tracking control part and enables the autonomous vehicle to perform human-like automated driving.

The perception system of an autonomous vehicle is composed of several types of sensors (e.g. Radar, Camera, Lidar, GPS, etc.). It provides the autonomy with surrounded environment information so as to execute decision making and planning process and guarantee the driving safety. In this paper, we assume that the ego vehicle equips a decent perception system which has the ability to observe and measure all the required environmental information. It should be noticed that the following figures and examples are based on left-hand traffic regulations (e.g. UK, JP, etc.).

Fig. 2 shows a basic traffic scenario while the vehicle is performing driving tasks, where P is the middle point of the vehicle rear axis; a is the lateral distance from point P to the right permitted border and d is the full permitted width which limits the active area of the vehicle. As mentioned previously, the request of executing 180 degrees turn cannot be expected in most instances and will have a higher priority. Hence, it is crucial to evaluate the feasibility of achieving the turn around target under the current environmental conditions and select the most convenient solution.

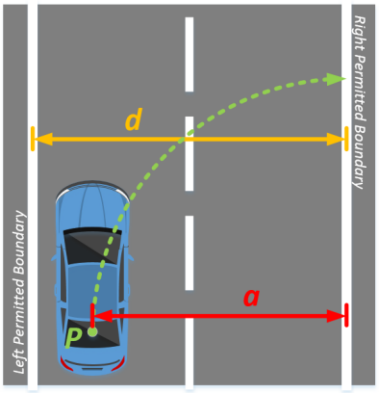

Fig. 2. A typical scenario while activating the turn around manoeuvre.

There is no doubt that a turn around manoeuvre can be treated as a high-risk activity since its operational area will overflow the current driving lane. As each transition between a forward and a reverse cornering costs a period of time, the 180 degrees turning with the less number of points is preferred to shorten the risk period. In order to realise the above functionalities, a general decision making framework is proposed in Fig. 3. D_1, D_3 and D_N represent the minimum utilised width of U Turn, Three-Point Turn and N-Point Turn respectively, where N is requested to be an odd number according to the property of multi-point turn.

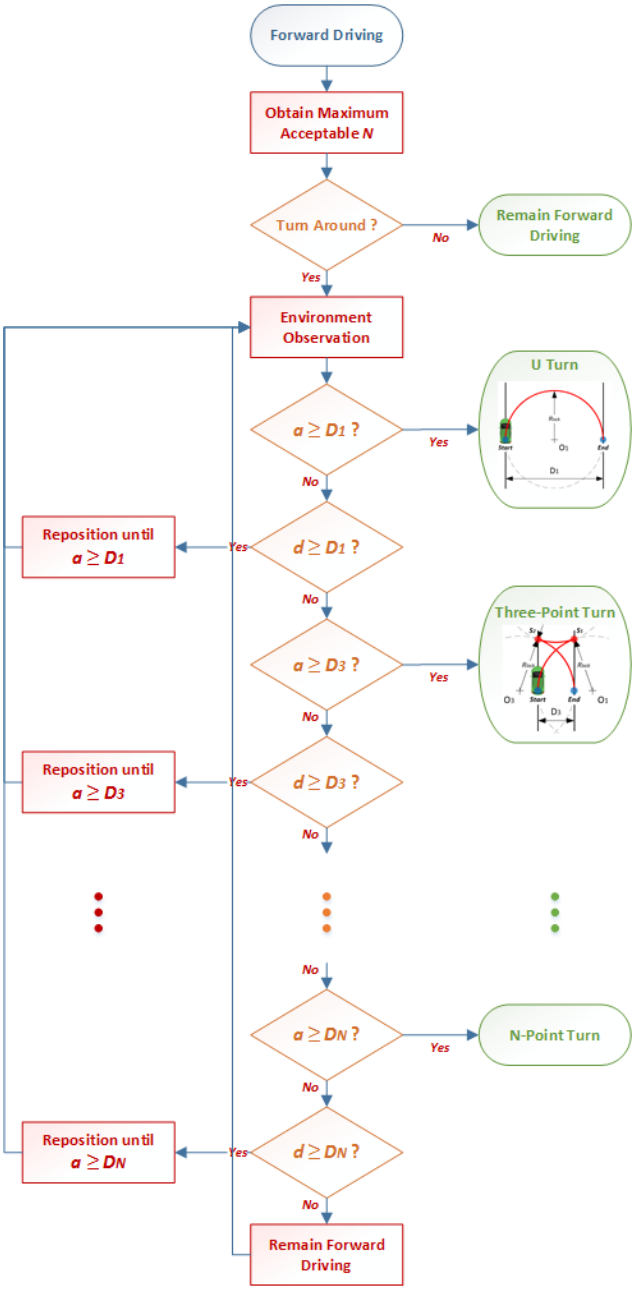

Fig. 3. The decision making framework for an autonomous vehicle to perform the most suitable turn around manoeuvre.

Starting with normal forward driving, the vehicle autonomy is assumed to be able to determine the necessity of turn around and the maximum acceptable value of N referring to the traffic conditions, the vehicle dimensions and the passenger's command. Once the request has been approved, both the full width d and the lateral distance a between P and the right boundary will be measured by the vehicle perception sensors. If a is equal to or greater than D_1, a U Turn will be selected and executed from the current position; if a is less than D_1 but d is equal or greater than D_1, the vehicle will remain forward driving and reposition its location until the new a is equal to D_1 in order to operate a U Turn from the new location. The same strategy is evaluated in selecting Three-Point Turn up to maximum acceptable N-Point Turn. Considering the preference of passengers and the constraints of vehicle dimensions, the vehicle is asked to remain forward driving if d cannot support the maximum acceptable N-Point Turn. This forward driving stage will be maintained until the new d is equal or greater than one of $D_1, D_3, \ldots, D_N$.

III. Analysis of the Turn Around Manoeuvres

This section illustrates and derives the narrowest requested road width D_1, D_3, D_5 and D_N, and the optimal reference paths that are based on geometric circles for a vehicle to achieve turn around tasks. To simplify the problem, the ego vehicle is considered as a point model (i.e. the point P in Fig. 2); and its heading direction is required to converse (i.e. turn 180 degrees) to complete the manoeuvre. A turn around manoeuvre comprises one or more forward and backword movements (Exception: U Turn is formed with only one forward movement); and will occupy the adjacent area which might be the oncoming traffic lane. Considering the safety and the efficiency, we assume that the hand steering wheel is steered to either the left or the right full lock position with cornering radius R_{lock} during each forward or backward driving; where R_{lock} can be calculate from the turning circle provided by car manufacturer. Moreover, the left and the right road boundaries are assumed to be two parallel lines and the turn around mission has to be operated within the area.

A. Geometric Properties and Constraints

The hand steering wheel (e.g. Ackermann Steering Angle in the Bicycle Model) controls the vehicle cornering radius and the driving path. As the hand steering wheel continues inputting the full lock steering signal while turning, the driving path becomes an arc or a circumference of the circle which has radius R_{lock}. Therefore, three geometry-related properties and constraints are depicted below.

1) Remark 1: The reference path of N-Point Turn is formulated by N arcs from N different circles, where N is an odd number.

2) Remark 2: Two circles that govern the sequential path pieces for a vehicle to converse the cornering direction are "tangented" at the transition point, at which the vehicle is requested to stop and manipulate the hand steering wheel to the opposite full lock position. Hence, the centres of the two circles are symmetric with each other to the transition point.

3) Remark 3: Each forward or reverse cornering has the ability to adjust the heading direction of the vehicle. With the purpose of finding the narrowest operation width, the process of executing a N-Point Turn has to get the utmost out of the available space. In other words, the start, the end and the transition points of the reference path have to be placed on either the left or the right road borders.

B. U Turn (N=1)

To converse the heading direction of a vehicle, U Turn is the simplest and most efficient solution a driver can operate, as shown in Fig. 4a. The reference path of U Turn can be treated as the arc of a semicircle with radius r if the steering angle is fixed. With manipulating the hand steering wheel at the full

lock position ($r = R_{lock}$) while cornering, the minimum threshold of the road width D_1 for a vehicle to perform a U Turn can be acquired as in (1).

$$D_1 = 2r = 2R_{lock} \quad (1)$$

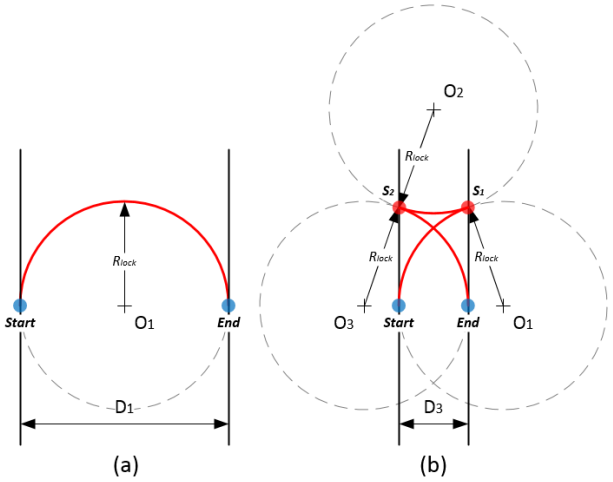

Fig. 4. The reference path (red curves) and the narrowest requested road width of (a) U Turn and (b) Three-Point Turn.

C. *Three-Point Turn (N=3)*

Although U Turn is preferable to other turn around manoeuvres, it might not be suitable under normal driving scenarios. The primary reason is that the driving path of U Turn will cross more than two standard traffic lanes, but the permitted width for a vehicle to converse the driving direction is often less than D_1. In order to achieve the turn around task within the above situation, the vehicle has to be stopped before breaking through the right road boundary and made a reverse with opposite steering but not to exceed the left road boundary; once the lateral distance to the right road boundary could afford the remaining turning, the vehicle makes the second stop and performs another forward cornering to finish the turn around manoeuvre, which is known as Three-Point Turn.

In general, Three-Point Turn comprises two forward and one reverse cornering. According to the geometric properties and the full lock position steering assumption, the reference path of Three-Point Turn can be decomposed into the arcs from three different circles with same radius R_{lock}. Fig. 4b depicts the scenario of utilising the narrowest road width to operate a Three-Point Turn, where O_1, O_2, and O_3 are the centres of circles that guide the vehicle to drive from the start point to the right road boundary, reverse to the left road boundary, and finalise the remaining cornering respectively; S_1 and S_2 are the vehicle stop points (i.e. transition points) at the right and the left road boundaries; D_3 is the minimum requested road width to implement a Three-Point Turn. Note that the points O_1, *End*, *Start* and O_3 are on the same line which is vertical to the road direction.

To find D_3, the line $\underline{O_1Start}$ and the line $\underline{O_3End}$ are first discussed; both their lengths are equal to R_{lock}. Accordingly, the lengths of the line $\underline{O_1End}$ and the line $\underline{O_3Start}$ are equal, and can be acquired as ($R_{lock} - D_3$). Considering the properties of congruent triangles, the lateral distances from O_2 to the left and the right road boundary can be determined, which also illuminate the relation between D_3 and R_{lock}, as shown in (2).

$$D_3 = 2R_{lock} - 2D_3 = 2R_{lock} / 3 \quad (2)$$

D. *Five-Point Turn (N=5)*

Five-Point Turn is another possible strategy to complete the turn around mission. It will consume more time, but can be applied to the situation which the permitted width is narrower than the minimum threshold D_3 of Three-Point Turn. The reorientation sequence for Five-Point Turn requires an additional forward and an additional backward cornering to compensate for the diminished width, since the maximum achievable turning angle of each path piece (e.g. from *Start* to S_1, from S_1 to S_2, etc.) is reduced.

In other words, the arcs from five different circles formulate the reference path of Five-Point Turn, including three forward and two reverse turnings. Taking the geometric properties and the aforementioned assumptions into account, a specific distribution of the five circles with same radius R_{lock} is able to minimise the occupied width, which is illustrated in Fig. 5. O_1, O_2, O_3, O_4 and O_5 are the centres of the above circles that guide the vehicle to complete the turn around manoeuvre. S_1 and S_3 are the transition points when the vehicle reaches the right border during the Five-Point Turn; S_2 and S_4 are the ones at the left border. D_5 is the lateral distance that represents the lower limit of the available width to perform a Five-Point Turn. Similar to Fig. 4b, the points O_1, *End*, *Start* and O_5 can be connected to form the line that is vertical to the left and the right operation borders.

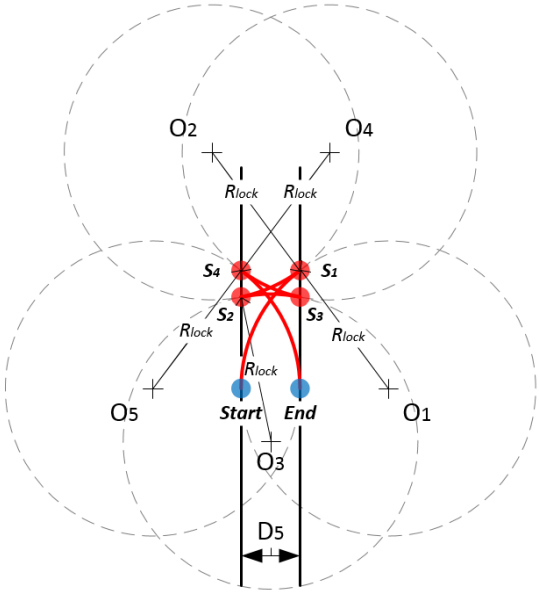

Fig. 5 The reference path (red curves) and the narrowest requested road width of Five-Point Turn.

The length D_5 can be obtained through deriving the side lengths of the congruent triangles. Start with calculating the lengths of the line $\underline{O_1End}$ and the line $\underline{O_5Start}$, which are both equal to ($R_{lock} - D_5$) and confirm the lateral distances from O_2

to the right boundary and from O_4 to the left boundary. By subtracting D_5 from the results, both the lateral distance between O_2 and the left boundary and the lateral distance between O_4 and the right boundary can be acquired as (R_{lock} – $2D_5$). Owing to the equivalent distances of the line $\underline{O_2S_2}$, the line $\underline{O_3S_2}$, the line $\underline{O_4S_3}$ and the line $\underline{O_3S_3}$ which are equal to the full lock cornering radius R_{lock}, these line are able to form another two pair of congruent triangles with the left and the right boundaries. Hence, the lateral distances from O_3 to the left and the right operational boundary can be determined in the meantime. Accordingly, the summation of these two distances (i.e. the lateral distances from O3 to the left and the right operational boundary) generates the outcome of the length D_5, and the relation is stated in (3).

$$D_5 = 2R_{lock} - 4D_5 = 2R_{lock} / 5 \tag{3}$$

E. N-Point Turn

The operational tactic of N-Point Turn is similar to Three-Point Turn and Five Point Turn: the vehicle starts with the forward cornering from a certain position, and recursively adjusts its heading direction through numerous forward and reverse reorientations within the permitted space (i.e. between the left and the right boundary) until the remaining turning can be achieved by the final forward cornering without breaking the right boundary.

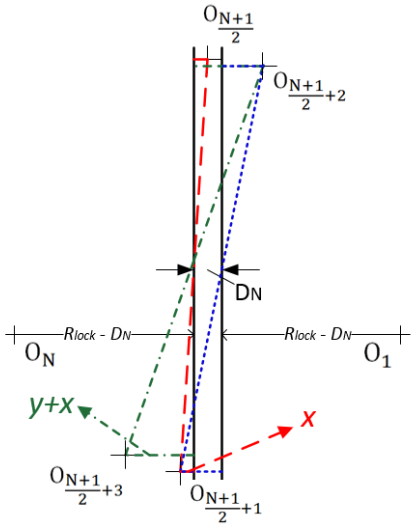

Fig. 6 The chart of deriving the min. operation width of N-Point Turn.

According to the distribution patterns from U Turn to Five-Point Turn, several regulations were observed and can be utilised to solve the narrowest operation width D_N for N-Point Turn. First, the reference path of N-Point Turn is composed of N arc pieces which are belong to N different circles with same radius R_{lock}. Moreover, the centres of the initial circle and the final circle (i.e. O_1 and O_N) can be connected by extending the line $\underline{StartEnd}$, which is vertical to the road direction. Then, the functionality of No.[(N + 1)/2] circle is to bridge the vehicle heading direction from less than 90 degree to over 90 degree (the heading direction at the start point and the end point are defined as degree 0 and degree 180 respectively); and the centre of this circle is located at a point on the central line of the road. On the other hand, the coordinates of two sequential centres (e.g. $O_{[(N+1)/2]}$ and $O_{[(N+1)/2+1]}$) are symmetric to their transition point with distance R_{lock}, which the point is on either the left or the right border.

Fig. 6 shows the draft distribution of sequential centres near the operation area, where O_1 to O_N are the centres of circles that provide N arc pieces to form the reference path of N-Point Turn. We first assume the lateral distance from $O_{[(N+1)/2+1]}$ to the left border is x, and the lateral distance between $O_{[(N+1)/2+1]}$ and $O_{[(N+1)/2+3]}$ is y. In order to calculate x and y, the properties of congruent triangles have to be applied. By focusing on the red congruent triangles, the distance between $O_{[(N+1)/2]}$ and the left border has the same length with x and is shown in (4). The blue congruent triangles illustrate that the width from $O_{[(N+1)/2+1]}$ to the right border is equal to the width from $O_{[(N+1)/2+2]}$ to the right border, which is (x + D_N). Furthermore, the green congruent triangles determine that the lateral distance from $O_{[(N+1)/2+2]}$ to the left border has the same length (x + $2D_N$) with the width between $O_{[(N+1)/2+3]}$ and the left border, which can be expressed as y + x. Consequently, the relation between y and D_N can be stated in (5).

$$x = D_N / 2 \tag{4}$$

$$y = 2D_N \tag{5}$$

The above procedures are derived recursively so as to compute the lateral distances between every two adjacent centres from $O_{[(N+1)/2+1]}$ to O_N, which are all equal to y. Hence, the lateral distance from O_N to the left border (i.e. R_{lock} – D_N) can be expressed by x and y, and the equation is stated in (6). Combing these three equations (i.e. (4), (5) and (6)), the narrowest occupied width D_N of N-Point Turn can be expressed by the cornering radius R_{lock}, as in (7).

$$R_{lock} - D_N = [\frac{N - (\frac{N+1}{2} + 1)}{2}] * y + x \tag{6}$$

$$D_N = 2R_{lock} / N \tag{7}$$

The validity of D_N can be confirmed by comparing the outcomes of aforementioned D_1, D_3 and D_5 in (1), (2) and (3). Note that Fig. 6 only presents the situation that $O_{[(N+1)/2]}$ is above the line $\underline{O_1O_N}$; the opposite situation (i.e. $O_{[(N+1)/2]}$ is below the line $\underline{O_1O_N}$) can be derived with the similar techniques and will deliver the same result as in (7).

IV. Discussions

Based on the relationship between the minimum occupied width of N-Point Turn that has been derived in the previous section and the vehicle full lock steering radius, we intends to form the functions which have the ability to continuously evaluate the most feasible turn around manoeuvre under current traffic conditions. Since the number of partitions during reorienting has to be odd numbers to complete a 180 degree turning, $\boldsymbol{O}$ is first defined as the set of the positive odd numbers, as shown in (8).

$$\boldsymbol{O} = \{\, m \mid m = 2n + 1 \,,\, n \in \boldsymbol{N} \,\} \tag{8}$$

Considering the proposed turn around decision making framework in Fig. 3, the environment observation process will be activated once the turn around manoeuvre is approved. Therefore, the lateral distance from the current position to the right available boundary (i.e. a) and the full permitted width (i.e. d) can be measured and provided as known variables to the targeted functions. Through inputting these two variables and the vehicle minimum cornering radius R_{lock} which can be acquired from the vehicle dynamic data to (9) and (10), the function f_1 is able to compute the minimum number of partitions of N-Point Turn that can achieve the turn around mission; the latter function f_2 will provide the result while considering the full permitted width.

$$f_1 (R_{lock} , a) = min \{ k \in \boldsymbol{O} | k \geq (2R_{lock} / a) \} \quad (9)$$

$$f_2 (R_{lock} , d) = min \{ k \in \boldsymbol{O} | k \geq (2R_{lock} / d) \} \quad (10)$$

According to the derivation outcomes in Section Three, (1), (2), (3), and (7) indicate that the minimum required widths of different turn around manoeuvres only depend on its partition number and the minimum cornering radius of the vehicle. The reason is that the ego vehicle is assumed and treated as a point-mass model in this paper, but it occupies a certain volume and cannot be neglected in reality. Hence, the work of re-analysing the vehicle from a point-mass model to a more complex model (e.g. bicycle model, four wheel model, etc.) and extending the outcomes of this paper to meet the realistic requirements will be focused in the next stage.

V. Conclusions And Future Work

This paper proposes a new framework of achieving human-like automated driving, which combines the real human driving data and the vehicle-dynamics-based motion planning. A general turn around decision making is then suggested, which can be referred while an autonomous vehicle intends to perform a turn around manoeuvre. The geometric characteristics that are followed by the reference paths of turn around manoeuvres are also analysed. Following with investigating the minimum operation widths from U Turn to Five-Point Turn respectively, the methodology and results are generalized to the N-Point Turn. Lastly, the derivative results and characteristics analysed above are treated as the input variables so as to formulate the functions that are able to evaluate the most feasible turn around manoeuvre within the current situation. Currently, the team is conducting multi-point turn road testing by different human drivers, characterising driving styles, and developing algorithms for multi-point turn decision making, path planning and tracking control for human-like automated vehicles.

References

[1] N. A. Stanton and M. S. Young, "Vehicle automation and driving performance," Ergonomics, vol. 41, no. 7, pp. 1014–1028, 1998.

[2] F. Y. Wang, X. Wang, L. Li, et al, "Steps toward parallel intelligence," IEEE/CAA Journal of Automatica Sinica, vol. 3, pp. 345–348, 2016.

[3] C. M. Martinez, X. Hu, D. Cao, E. Velenis, B. Gao, and M. Wellers, "Energy management in plug-in hybrid electric vehicles: recent progress and a connected vehicles perspective," IEEE Transactions on Vehicular Technology, vol. 66, pp. 4534–4549, 2017.

[4] F. Y. Wang, J. Zhang, Q. Wei, X. Zheng, and L. Li, "PDP: parallel dynamic programming," IEEE/CAA Journal of Automatica Sinica, vol. 4, pp. 1–5, 2017.

[5] X. Li, Z. Sun, D. Cao, Z. et al, "Real-time trajectory planning for autonomous urban driving: Framework, Algorithms, and Verifications," IEEE/ASME Transactions on Mechatronics, vol. 21, pp. 740–753, 2016.

[6] H. Guo, J. Liu, D. Cao, H. Chen, R. Yu, and C. Lv, "Dual-envelop-oriented moving horizon path tracking control for fully automated vehicles," Mechatronics, 2017.

[7] F. Y. Wang. "Control 5.0: from Newton to Merton in popper's cyber-social-physical spaces." IEEE/CAA Journal of Automatica Sinica, vol. 3, pp. 233–234, 2016.

[8] E. Rosén, J. E. Källhammer, D. Eriksson, M. Nentwich, R. Fredriksson, and K. Smith, "Pedestrian injury mitigation by autonomous braking," Accid. Anal. Prev., vol. 42, no. 6, pp. 1949–1957, 2010.

[9] X. Li, Z. Sun, D. Cao, D. Liu, and H. He, "Development of a new integrated local trajectory planning and tracking control framework for autonomous ground vehicles," Mechanical Systems and Signal Processing, vol. 87, pp. 118–137, 2017.

[10] C. Lv, H. Wang, and D. Cao, "High-Precision Hydraulic Pressure Control Based on Linear Pressure-Drop Modulation in Valve Critical Equilibrium State," IEEE Transactions on Industrial Electronics, 2017.

[11] L. Li, Y. Lv, and F. Y. Wang, "Traffic signal timing via deep reinforcement learning," IEEE/CAA Journal of Automatica Sinica, vol. 3, pp. 247–254, 2016.

[12] L. Li, W. L. Huang, Y. Liu, N. N. Zheng, and F. Y. Wang, "Intelligence Testing for Autonomous Vehicles: A New Approach," IEEE Transactions on Intelligent Vehicles, vol. 1, pp. 158–166, 2016.

[13] C. Diels, "Will autonomous vehicles make us sick?," Contemp. Ergon. Hum. Factors, pp. 301–307, October 2014.

[14] M. Elbanhawi, M. Simic, and R. Jazar, "In the passenger seat: investigating ride comfort measures in autonomous cars," IEEE Intell. Transp. Syst. Mag., vol. 7, no. 3, pp. 4–17, 2015.

[15] M. Sivak, B. Schoettle, "Motion sickness in self-driving vehicles," 2015.

[16] C. Diels and J. E. Bos, "Self-driving carsickness," Appl. Ergon., vol. 53, pp. 374–382, 2015.

[17] W. Nelson, "Continuous-curvature paths for autonomous vehicles," Int. Conf. Robot. Autom., pp. 1260–1264, 1989.

[18] Y. Kuwata, J. Teo, G. Fiore, et al, "Real-time motion planning with applications to autonomous urban driving," IEEE Trans. Control Syst. Technol., vol. 17, no. 5, pp. 1105–1118, 2009.

[19] Y. Chen and S. Yasunobu, "Soft target based obstacle avoidance for car-like mobile robot in dynamic environment," IEEE Int. Conf. Fuzzy Syst., 2007.

[20] Google, "Mastering the Three-Point Turn," Google Self-Driving Car Project Monthly Report, October 2016.

[21] J. Reeds and L. Shepp, "Optimal paths for a car that goes both forwards and backwards," Pacific J. Math., vol. 145, no. 2, pp. 367–393, 1990.

[22] X. Hu, L. Chen, B. Tang, D. Cao, H. He, "Dynamic path planning for autonomous driving on various roads with avoidance of static and moving obstacles," Mechanical Systems and Signal Processing, in press.

[23] H. Guo, J. Liu, R. Yu, D. Cao, H. Chen, "Dual-envelop-oriented moving horizon trajectory tracking control for fully automated vehicles," Mechatronics, in press.

[24] F. Wang, H. Chen, K. Guo, D. Cao, "A novel integrated approach for path following and directional stability control of road vehicles after a tire blow-out," Mechanical Systems and Signal Processing, vol. 93, pp. 431–444, 2017.

[25] G. Jia, L. Li, D. Cao, "Model-based estimation for vehicle dynamics states at the limit handling," ASME Journal of Dynamic Systems, Measurement and Control, 137 (10), 104501, 2015.

[26] C. M. Martinez, M. Heucke, F. Wang, B. Gao, D. Cao, "Driving style recognition for intelligent vehicle control and advanced driver assistance: a survey," IEEE Transactions on Intelligent Transportation Systems, in press.